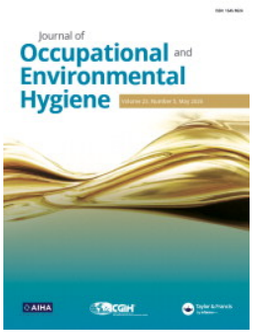

Journal of Occupational and Environmental Hygiene

ISSN: 1545-9624 (Print) 1545-9632 (Online) Journal homepage: www.tandfonline.com/journals/uoeh20

Real-time evaluation of workplace protection factors from powered air-purifying respirators

Xinyi Niu, Michael Yermakov, Matthew Horvatin, Ziqing Zhuang, Weihua Yang, Sergey Grinshpun & Jun Wang

To cite this article: Xinyi Niu, Michael Yermakov, Matthew Horvatin, Ziqing Zhuang, Weihua Yang, Sergey Grinshpun & Jun Wang (01 Jun 2026): Real-time evaluation of workplace protection factors from powered air-purifying respirators, Journal of Occupational and Environmental Hygiene, DOI: 10.1080/15459624.2026.2659848

To link to this article: https://doi.org/10.1080/15459624.2026.2659848

Published online: 01 Jun 2026.

JOURNAL OF OCCUPATIONAL AND ENVIRONMENTAL HYGIENE
https://doi.org/10.1080/15459624.2026.2659848

Real-time evaluation of workplace protection factors from powered air-purifying respirators

Xinyi Niu[a], Michael Yermakov[a], Matthew Horvatin[b], Ziqing Zhuang[b], Weihua Yang[c], Sergey Grinshpun[a], and Jun Wang[a]

[a]Department of Environmental and Public Health Science, College of Medicine, University of Cincinnati, Cincinnati, Ohio; [b]Policy and Standard Development Branch, National Institute for Occupational Safety and Health, National Personal Protective Technology Laboratory, Pittsburgh, Pennsylvania; [c]The Oak Ridge Institute for Science and Education (ORISE), Oak Ridge, Tennessee

ABSTRACT

Loose-fitting powered air-purifying respirators (PAPRs) are widely used by healthcare workers to protect against inhalation hazards, as they require no fit testing. However, incorrect use can compromise their efficacy, which may progressively deteriorate over time. Therefore, there is a critical need for real-time monitoring of PAPR performance during occupational activities. In this study, a portable device called the Exposure Protection Integrated Communicator (EPIC) was developed, which uses optical particle sensors to evaluate the workplace protection provided by PAPRs. EPIC monitors concentrations inside and outside a respirator using two sensors to quantitatively calculate the protection factor (PF), defined as the ratio of particle concentrations outside to inside the respirator. The system applied algorithms to correct sensor readings and alert wearers if respirator protection was compromised. The prototype EPIC was evaluated using a manikin headform connected to a breathing recording and simulation system (BRSS) to simulate a sinusoidal breathing pattern. A PortaCount fit tester based on a single-condensation-nuclei-counter principle served as the reference measurement device during parallel tests. The results were expressed as PFs for comparison between the EPIC system and the reference method. The prototype EPIC demonstrated to be an effective tool for quantifying the real-time performance of PAPRs, particularly in environments with particle concentrations of 40,000 to 70,000 particles/L. Data collected from both the EPIC and PortaCount were compared, revealing that the EPIC could measure PFs ranging from 10 to 10,000. The EPIC showed a strong correlation with the reference PortaCount ($R^2 = 0.84$), despite the two systems using different measurement principles and detection limits. The study results confirmed the effectiveness of EPIC in quantitatively assessing respirator particle ingress.

KEYWORDS

Optical particle sensor; PAPRs; workplace protection factor; healthcare workers; first responder

Introduction

Inhalation exposure to particles within the respirable and inhalable size fractions is commonly observed in occupational workplaces. Aerosols can be generated either through direct emissions or secondary resuspension (Nicholson 1988; Hinds 1999). These aerosolized particles may be toxic or contain pathogens, such as viruses, fungal spores, infectious bioaerosols, or bacteria, especially in healthcare environments (Wei and Li 2016; Zhai et al. 2018; Tellier et al. 2019). Healthcare workers (HCWs) are at high risk of occupational exposure to these aerosols (Mohanty et al. 2019). The outbreaks of emerging infectious diseases, such as the 2003 severe acute respiratory syndrome (SARS) outbreak, the 2014 Ebola Epidemic, and the Coronavirus disease 2019 (COVID-19) pandemic, have highlighted the risk of disease transmission among HCWs. It is estimated that approximately 20% of HCWs who cared for SARS patients became infected during the first SARS epidemic (Nicas et al. 2004). During infectious disease outbreaks, demand for personal protective equipment (PPE) can quickly outpace supply. Reusable respiratory protection can be a sustainable option, and elastomeric half-mask respirators have been proposed as a solution. Significant research has examined their application to healthcare settings. Powered air-purifying respirators may also be suitable alternatives.

PAPRs use a blower to draw ambient air through air-purifying elements into the helmet/hood inlet or a

CONTACT Jun Wang jun.wang@uc.edu Department of Environmental and Public Health Science, College of Medicine, University of Cincinnati, 160 Panzeca Way, Cincinnati, OH 45267.

tight-fitting facepiece, providing workers with protection against hazardous aerosolized particulates. PAPRs with loose-fitting inlet coverings are often preferred by HCWs over N95 FFRs, because they do not require fit testing and may offer greater comfort (Liverman et al. 2014). Additionally, loose-fitting PAPRs can be worn by individuals whose facial hair, facial coverings, and various facial structures may prevent a proper fit with N95 FFRs. Meanwhile, some loose-fitting PAPR hood designs fully cover the wearer's head and neck, providing additional protection against contact with body fluids (Grinshpun et al. 2020). As a result, the use of PAPRs is rapidly increasing across workplaces, and they are considered a viable option in some occupational settings, particularly for HCWs in public health emergencies when N95 FFRs are in short supply (Wizner et al. 2016).

The Occupational Safety and Health Administration (OSHA) mandates that PAPRs used in OSHA-regulated workplaces be approved by the National Institute for Occupational Safety and Health (NIOSH) under 42 CFR Part 84. OSHA specifies assigned protection factors (APF) of 25 or 1,000 for PAPRs with helmets/hoods (29 CFR 1910.134). An APF of 25 is designated as the default for helmets/hoods unless the manufacturer provides evidence that the PAPR protects at a level of 1,000 or greater (OSHA 2006). The respirator manufacturer shall provide evidence of such performance through workplace protection factor (WPF), simulated workplace protection factor (SWPF), or equivalent testing results (Myers et al. 1984, 1986; Cohen et al. 2001; Vo et al. 2015). The study from Cohen et al. (2001) showed that PAPRs can significantly exceed their APFs of 25 or 1,000, with some median SWPF values surpassing 250,000, suggesting the actual protection provided by PAPRs may be far greater than expected. However, in real-world workplace environments, factors such as the complexity of PAPRs, insufficient user training, and work-related constraints may lead to incorrect PAPR use, reducing their protective performance (Liverman et al. 2014). Generally, insufficient flow (over-breathing), design flaws (poor design and manufacturing defects), and improperly attached PAPR components (such as an untightened hose or an untucked bib) may also affect PAPR performance (Mackey et al. 2005; Gao et al. 2016).

Given the hazards in healthcare environments, including worker exposure to infectious aerosols and hazardous substances, continuous real-time PAPR performance monitoring can help promptly alert wearers to performance compromises. The WPFs and SWPFs are typically measured using condensation nuclei counters (CNCs), such as PortaCount (TSI Inc., Shoreview, MN) and similar instruments. While certain PortaCount models are portable and suitable for field use, they are relatively expensive and require consumables. They are not intended for continuous, real-time, wearable protection factor monitoring during routine respirator use, thereby limiting their practicality for ongoing field assessment efforts. Therefore, developing a low-cost, wearable tool capable of real-time monitoring of respirator performance can be useful and valuable. Such a tool needs to continuously monitor the PAPR's protection factors and alert wearers to potential compromises.

The Exposure Protection Integrated Communicator (EPIC), a novel prototype device for real-time monitoring of respirator performance, is an advanced version of the real-time performance monitor (RePM), which was considered to be the first device designed to quantitatively assess the performance of respirators such as PAPR and N95 FFRs during use (Grinshpun et al. 2020). Unlike formal WPF or SWPF testing conducted for regulatory or standardized evaluation purposes, EPIC is intended as a field decision-support tool that provides continuous, real-time feedback on respirator performance to help identify degradation of respirator protection factors during actual use, rather than to replace compliance-based assessments. Despite its initial innovativeness, the RePM had limitations, including a long response time (60 s), an inability to differentiate between particle sizes, and a lack of user interfaces for wearers (Grinshpun et al. 2020). The prototype EPIC addressed these shortcomings by offering faster response times, improved particle size detection, and a user-friendly interface. This study aimed to evaluate the EPIC's efficacy in measuring PAPR performance and compare its accuracy with that of existing CNC-based fit testers.

Methods

Concept and design of EPIC

The EPIC is equipped with a pair of optical particle sensors (PMS-11, Temtop Inc., San Jose, CA, USA) that operate on the principle of light scattering and can detect particulate size bins with median sizes of 0.3, 0.5, 0.7, 1.0, 2.5, and 5 μm. The PMS-11 sensor utilizes advanced processing chips and photosensitive elements, with signal capture and processing performed by an integrated microprocessor and output via a universal digital interface. The PMS-11 sensors can measure and report the mass and count of

airborne particles per unit air volume (L). The dual PMS-11 sensor configuration within the EPIC facilitates simultaneous measurement of aerosol concentrations inside and outside the respirator by being separately attached to the inlet and outlet of PAPRs via tubing connections. Thus, the EPIC framework represents a quantitative approach and offers advantages over a traditional fit tester single-particle count design. By measuring the inside aerosol concentration (C_{in}) and the outside aerosol concentration (C_{out}), respirator protection factors (PF) were calculated as

$$PF = \frac{C_{out}}{C_{in}} \quad (1)$$

EPIC is also equipped with a touch screen featuring a custom user interface for intuitive interaction. Data collected from the sensors can be wirelessly transmitted to a cloud environment via the Internet (e.g., Wi-Fi), enabling remote access and information processing. Additionally, the EPIC incorporates robust battery management to support continuous respirator use throughout a work shift and modular components for easy maintenance and replacement. The EPIC maintains a compact, wearable form factor by integrating inexpensive commercial sensors and low-cost peripheral components, while delivering excellent operational performance.

The EPIC unit offers two operating modes: an "easy" mode for the wearer and an "expert" mode for safety professionals or respiratory protection program managers. The easy mode provides essential information and alerts the wearer if the respirator's integrity is compromised, i.e., PFs fall below threshold values. The expert mode provides time-series data and allows data to be transferred wirelessly or downloaded to a USB drive for further analysis. The current EPIC prototype features a 3-color LED indicator system—red, yellow, and green—to represent various respirator protection factor thresholds. For example, the color coding for full-face PAPR was as follows: red indicates a PF less than 500, yellow denotes a PF of 500–1,000, and green signifies a PF of 1,000 or greater. Notably, in both "easy" and "expert" modes, EPIC displayed "CLEAR" rather than providing a specific PF value when the PAPR was worn correctly, indicating a very high protection factor.

However, the EPIC's performance is influenced by the principles and detection limits of the optical particle counting sensor. Thus, the experimental setup was specifically designed to evaluate and address these potential limitations.

Evaluation of EPIC

The prototype EPIC reduces response time compared to the previous generation RePM, from 60 s (Grinshpun et al. 2020) to 1.5 s. A series of validation and performance evaluation experiments was conducted on the tested PAPR donned on a manikin headform connected to a simulated breathing machine. The experiments were performed in a 24 m^3 chamber, with 1% concentrated sodium chloride (NaCl) as the challenge aerosol. NaCl was selected because it is widely used in controlled-chamber studies and serves as the standard challenge aerosol for respirator certification testing under *NIOSH 42 CFR Part 84* regulations (NIOSH 1997). The NaCl particles were generated using a 6 Jet collision nebulizer (MRE, 6 Jet Vertical, CH Technologies Inc., Westwood, NJ, USA), which produced particles ranging in size from nanometers to microns. The manikin-based setup and chamber setup are illustrated in Figure 1. The headform manikin was connected to a Breathing Recording and Simulation System (BRSS, Koken Ltd., Tokyo, Japan), containing an electromechanical drive and two air cylinders to simulate a sinusoidal breathing pattern of a human by adjusting the mean inspiratory flow (MIF) rates and breathing frequency (Haruta et al. 2008). Tests were conducted at three MIFs of 30, 85, and 135 L/min, which are regarded as three common breathing conditions representing medium, high, and strenuous workloads (Lafortuna et al. 1984; Anderson et al. 2006). The cylinder's movement distance within the BRSS simulates the human tidal volume by adjusting its speed and stroke distance. The breathing frequency was set to 0.25, 0.42, and 0.5, corresponding to different tidal volumes. The EPIC unit operated in parallel with a PortaCount Fit Tester (Model 8048, TSI Inc., Shoreview, MN, USA), serving as a reference method based on CNC. The PortaCount monitoring data were used to compare with the real-time results from the prototype EPIC, enabling the establishment of a correlation between PFs measured by both devices. The prototype EPIC was set to a sampling rate of 1.5 sec for real-time monitoring of PF values, which is relatively similar to the 1 sec response time of the PortaCount. The inside samples were collected near the mouth area inside the respirator, and the outside samples were collected within 30 cm of the mouth outside the respirator.

The three NIOSH-Approved PAPR models tested were PAPR A, PAPR B, and PAPR C. The manufacturer information, including PAPR and hood models and brands, is not disclosed to ensure impartiality and prevent unintentional endorsement or dissemination of product-specific information. PAPR B operated at 184 and 204 L/min flow rates, and PAPR C offered

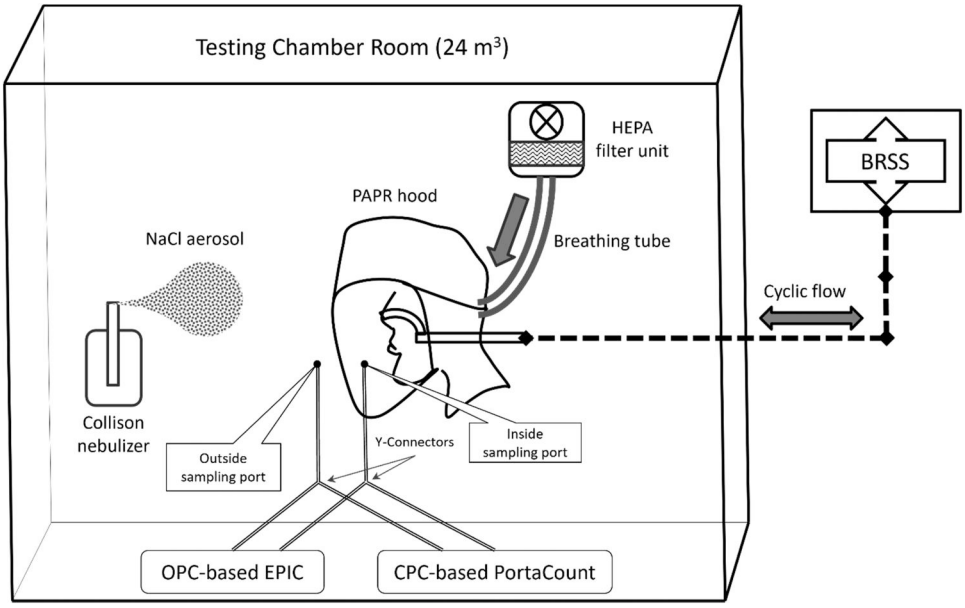

Figure 1. Schematic diagram of the manikin-based chamber setup.

Table 1. NIOSH-approved powered air-purifying respirators (PAPRs) paired with their corresponding hoods.

PAPRs	Flow rates	Hoods
PAPR A	0 ~ 175 L/min	Hood A (Regular size) and Hood B (Large size)
PAPR B	184 and 204 L/min	
PAPR C	170, 210, and 240 L/min	Hood C (Medium/Large size)

three motor/blower modes at 170, 210, and 240 L/min. PAPR A was equipped with an additional knob that allows the user to adjust flow rates from 0 to 175 L/min. This extra knob simulated a partially discharged PAPR unit battery, enabling lower flow rates that would be generated by a PAPR with a low battery. The adjustment knob, located outside the HEPA filter housing, regulated the voltage supplied to the blower motor, which, in turn, controlled the PAPR A flow rate. Changing the voltage permitted adjustment of the PAPR A flow rate, with a minimum flow rate of 80 L/min at 2.3 V and a normal flow rate of ~210 L/min, corresponding to a fully charged battery at 4.8 V.

Three hood models were evaluated in conjunction with PAPRs: Hood A (Regular size), Hood B (Large size), and Hood C (Medium/Large size). Both hoods A and B were compatible with the PAPRs A and B, whereas Hood C can be used with PAPR C. Table 1 presents the tested PAPRs and their corresponding hood models. All tested hoods were equipped with inner collars and premium head suspensions, which were available to don on the manikin headform during the experiments.

Parallel testing was performed by PAPR A to determine the correction factor (CF) between PF_{EPIC} and $PF_{PortaCount}$ at different ambient particle concentrations. Hood A, with a regular size, was donned on the manikin headform. The parallel testing was performed on the working PAPR A without BRSS operating. The PAPR's flow rate was adjusted to achieve three stable PFs of 10, 50, and 100, which were measured using the reference PortaCount Fit Tester. The correction factor (CF) was determined by the ratio of the PF measured by the reference device and EPIC prototype, as shown in Equation 2:

$$CF = \frac{PF_{PortaCount}}{PF_{EPIC}} \quad (2)$$

The order of the experimental conditions under which the EPIC prototype was evaluated was randomized. These experiments tested different airflow conditions by adjusting PAPR flow rates and simulated different breathing rates, aiming to generate a broad range of protection factor values for comparison between the EPIC and PortaCount. These variations were reported to affect the performance of the inside sampling port and to require thorough testing (Haruta et al. 2008). Each combination of PAPR flow rates and simulated breathing rates was replicated at least 3 times to ensure adequate statistical power. Two-tailed *t*-tests were performed to compare the performance of EPIC and PortaCount across varying

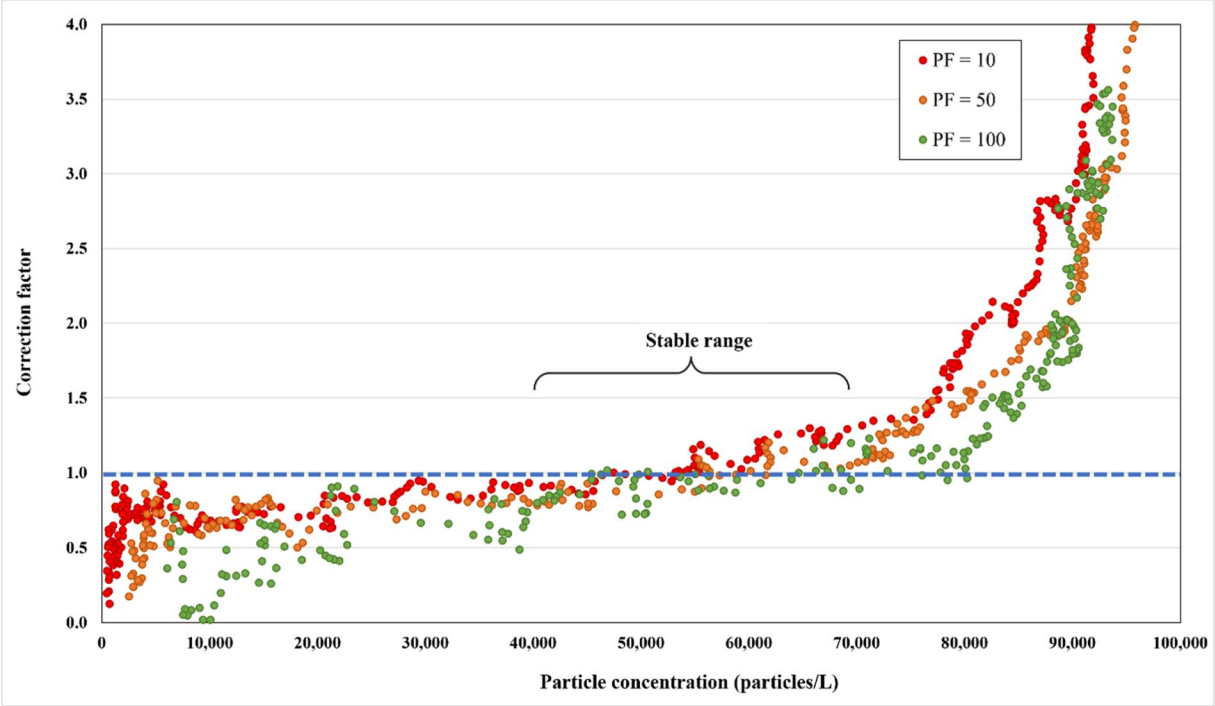

Figure 2. Correction factors (CF) between the PF_{EPIC} and $PF_{PortaCount}$ at different ambient particle concentrations. Three stable PF values of 10, 50, and 100 measured by PortaCount were achieved by adjusting the flow rates of the tested PAPR A. Particle concentrations (particles/L) were measured by the EPIC optical light-scattering sensor.

experimental conditions ($p < 0.05$). Normality of the differences was assessed using the Shapiro-Wilk test ($p < 0.001$), indicating that the differences were not normally distributed; therefore, a Wilcoxon signed-rank test was performed, which showed no significant difference between the EPIC and reference measurements ($W = 1036.0$, $p = 0.058$).

Results and discussion

Correction factors for EPIC

A diagram illustrating the CFs between the PF_{EPIC} and $PF_{PortaCount}$ at different ambient particle concentrations is shown in Figure 2. Three stable PF values of 10, 50, and 100 were measured by PortaCount by adjusting the flow rates of the tested PAPR. The results reveal that the prototype EPIC operated effectively across a broad range of particle concentrations, from low (~4 particles/L) to high (>100,000 particles/L). Across all three tested PF levels, CF increased with rising ambient particle concentration, indicating that CF was primarily dependent on ambient particle concentration within the evaluated range. Specifically, the CF remained below 1.0 at ambient concentrations below 40,000 particles/L, approached 1.0 in the medium concentration range of 40,000 to 70,000 particles/L, and exceeded 1.0 at concentrations above 70,000 particles/L. The discrepancy between the EPIC and PortaCount measurements was minimal at medium ambient particle concentrations. Therefore, the manikin-based evaluations were conducted at ambient concentrations ranging from 40,000 to 70,000 particles/L, within the stable range where the two instruments showed the most consistent agreement, as indicated in Figure 2.

The parallel testing conducted with the EPIC PMS-11 sensor yielded a minimum aerosol concentration of ~ 4 particles/L, surpassing the lower limit of 300 particles/L established by RePM (Wu et al. 2018). This lower limit enabled more accurate monitoring of clean air inside a functioning respirator. The highest concentration tested by the EPIC PMS-11 sensor was ~90,000 particles/L. While the lower detection limit has been improved, the upper limit remains about 50% of the RePM's upper value, which was 200,000 particles/L (Wu et al. 2018). The range of 4 to 90,000 particles/L demonstrated that EPIC offers enhanced sensitivity at lower concentration thresholds, but challenges persisted in monitoring high levels of contamination in the air.

The higher the ambient concentration, the larger the CF was for ambient particles (particles outside the respirator), with a CF of 70,000 particles/L or higher indicating the most significant difference between EPIC and reference PortaCount at high particle

concentrations. This difference may be attributed to the different working principles of the particle counting sensors. The PortaCount fit tester employs a CNC principle to detect and count aerosol particles by enlarging through saturated vapor condensation before measurements. The prototype EPIC, based on the optical light-scattering principle, may produce inaccurate readings at high particle concentrations due to simultaneous scattering from multiple particles within the sensing volume. Meanwhile, the output of optical light-scattering sensors is sensitive to the refractive index of particles, which varies with their composition. While the correction factor presented in Figure 2 may vary depending on particle compositions, sizes, and the effects of the tested environment's temperature and relative humidity (RH) on the particle sensor, the key finding is that a relationship between outputs was established for EPIC and particle concentration (Wang et al. 2015; Sousan et al. 2017).

EPIC evaluation at varying PAPR airflows

The ambient particle concentrations in the test chamber were controlled within 40,000 to 70,000 particles/L, which was a stable range for EPIC, and therefore, the use of CFs was not necessary. Figure 3 presents the respirator PF values measured with EPIC and PortaCount for two types of PAPRs: PAPR A with Hood A and PAPR C with Hood C, both donned on a headform manikin under an MIF of 135 L/min. Results showed that a tidal volume of 2.2 L produced significantly ($p < 0.05$) higher PF values compared to the 2.7 L tidal volume, indicating the larger tidal volume may result in a lower PF at the same MIF. The lower PF at higher tidal volumes may be attributed to prolonged airflow duration, which can generate increased air turbulence within the respirator, potentially compromising the face seal and reducing overall protection. Significant differences ($p < 0.05$) between EPIC and PortaCount were observed at PAPR flow rates of 110, 125, and 135 L/min. However, no significant differences were observed at higher flow rates, suggesting that EPIC may maintain comparable accuracy at elevated PAPR.

For both tested PAPRs, the PF values increased with higher fan flow rates, indicating improved protection at higher flow rates. At both tested tidal volumes, the PF values measured by EPIC were lower than those recorded by PortaCount, but the differences were not significant. At high tidal volumes, smaller particles may penetrate the filter (Mahdavi et al. 2014; Gao et al. 2015), and the EPIC system, which uses optical light-scattering for particle counting, may be less sensitive to detect these smaller particles inside the respirator, potentially leading to an overestimation of PF compared to the PortaCount that employs condensation nuclei counting. Future research is warranted to determine the particle size range at which the EPIC system begins to diverge from the PortaCount in performance.

In addition, the performance of EPIC was evaluated using PAPR A at a tidal volume of 2.7 L and a PAPR flow rate of 110 L/min, with varying MIFs. This was aimed at assessing the impact of MIF on respirator protection factors and comparing the performance of EPIC and PortaCount across different MIFs. The PAPR flow rate of 110 L/min was selected because it produced a relatively low PF within the detection range of both measurement devices. MIFs of 30, 85, and 135 L/min were chosen to represent medium, high, and strenuous workloads (Lafortuna et al. 1984; Anderson et al. 2006). The respirator PF values measured with the EPIC and PortaCount for PAPR A with Hood A donned on a headform manikin under different MIFs are presented in Figure 4. Results show that EPIC reported significantly ($p < 0.05$) higher PF values than PortaCount at low and moderate MIFs. However, the difference between the PF_{EPIC} and $PF_{PortaCount}$ was not statistically significant at the high MIF, with EPIC reporting slightly lower PF values than PortaCount.

These findings suggest that EPIC reliably measured respirator PFs under high MIF conditions and maintained performance comparable to that of the reference PortaCount. The respirator's filtration efficiency was generally higher at lower flow rates because the filter material experienced less stress, resulting in reduced particle penetration. Since EPIC primarily detected larger particles, it may have reported higher PF values under these conditions, as the respirator effectively blocks these particles. However, at higher MIFs, the filter is subjected to greater strain, allowing particles to penetrate the respirator. Both EPIC and PortaCount detected more particles, and their readings became more similar at higher MIFs, leading to non-significant ($p > 0.05$) differences in PF measurements between the two devices.

EPIC evaluation on varying hood donnings

Hoods with different coverage gaps were separately attached to the PAPR B and tested on a headform manikin to evaluate the EPIC performance. The hoods

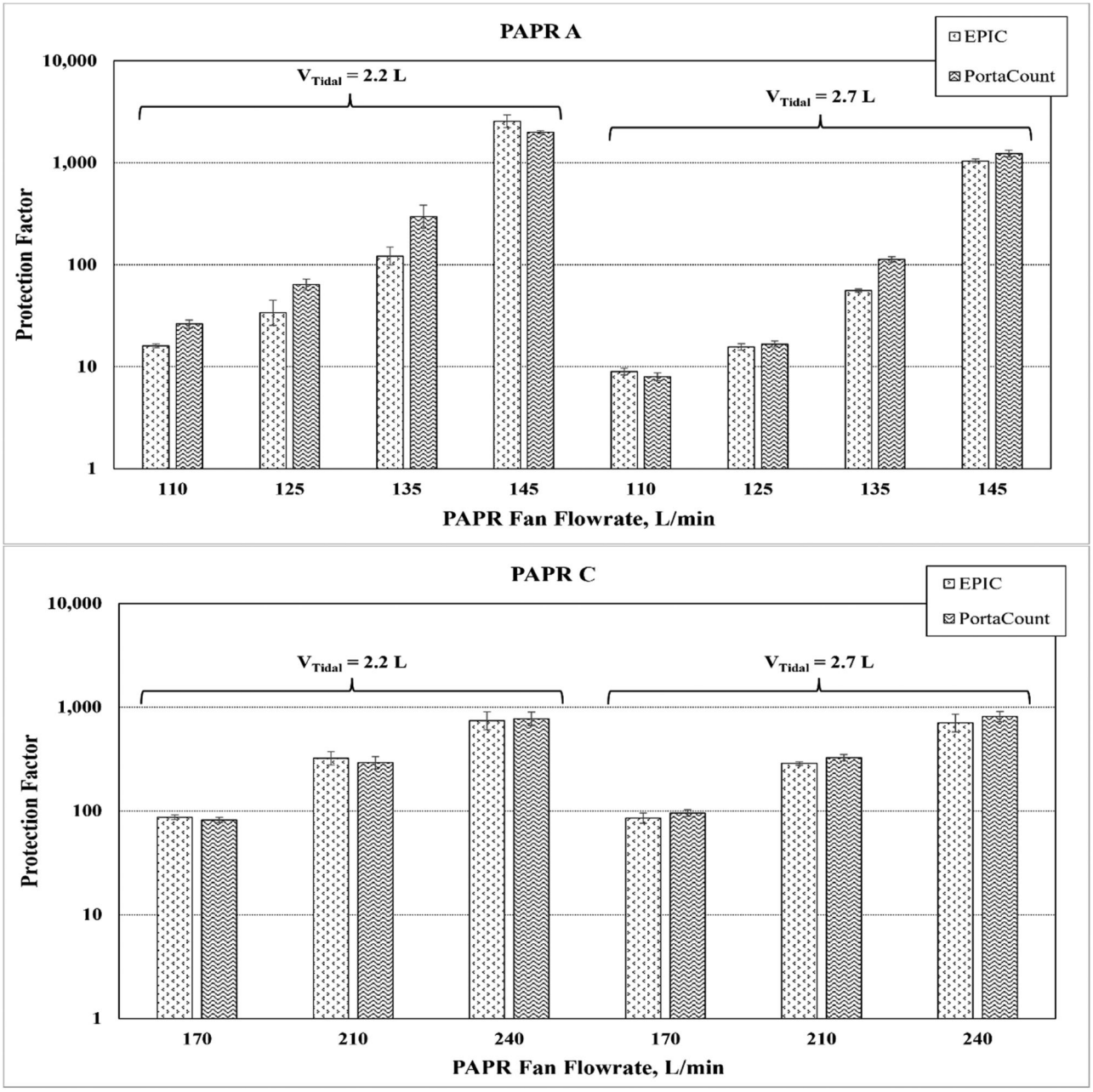

Figure 3. Respirator protection factors (PF) measured with EPIC and PortaCount for two types of PAPRs: PAPR A with Hood A and PAPR C with Hood C donned on a headform manikin under a mean inspiratory flow rate (MIF) of 135 L/min. The bars represent the geometric mean of PF values determined under different tidal volumes and PAPR flow rates. The error bars represent geometric standard deviations of PF values on a log scale.

tested included Hood A (Regular size), Hood B (Large size), and Hood B with a stretched elastic band. PAPR B offered two adjustable flow rates of 184 and 204 L/min. Figure 5 presents the respirator PF values measured with EPIC and PortaCount for the PAPR B with varying hood coverage gaps donned on the headform manikin. Measurements were taken at an MIF of 135 L/min and a tidal volume of 2.7 L across different PAPR flow rates. The PF values recorded from Hood A exceeded 30,000, and EPIC displayed "CLEAR" instead of providing the specific PF values. Therefore, Figure 5 shows only the PF values for Hood B (not stretched) and Hood B with the stretched elastic band.

The Hood B with the stretched elastic band produced significantly lower protection factors ($p < 0.05$) than the conventional Hood B (not stretched). For Hood B, the PF values measured by EPIC were significantly ($p < 0.01$) higher than those measured by PortaCount at both PAPR's flow rates. However, no significant difference was found between PF_{EPIC} and

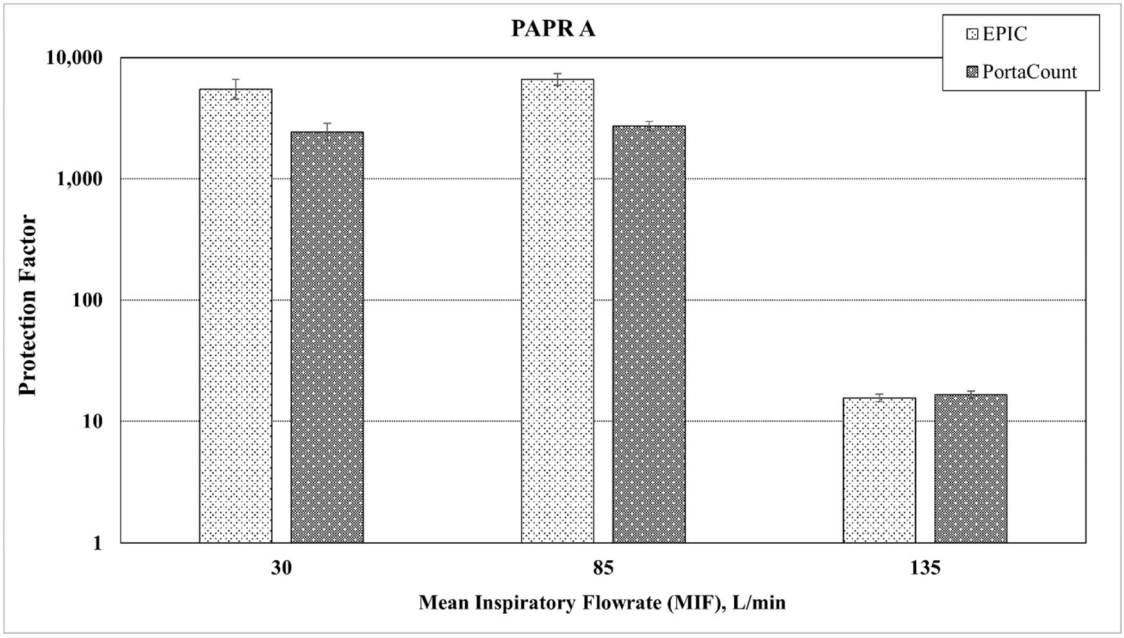

Figure 4. Respirator protection factors (PF) were measured with EPIC and PortaCount for PAPR A with Hood A donned on a headform manikin under different mean inspiratory flow rates (MIFs) of 30, 85, and 135 L/min. The bars represent the geometric mean of PF values determined under a tidal volume of 2.7 L and a PAPR flow rate of 110 L/min. The error bars represent geometric standard deviations of PF values on a log scale.

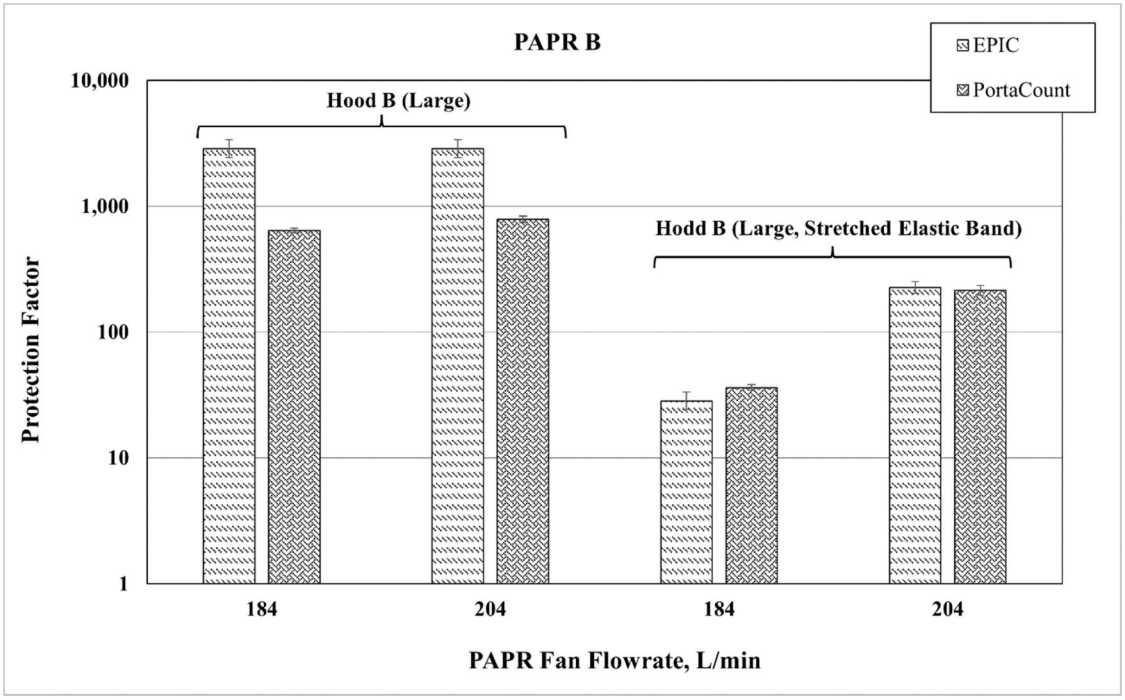

Figure 5. Respirator protection factors (PF) were measured with EPIC and PortaCount for PAPR B with varying hood coverage gaps donned on a headform manikin under a mean inspiratory flow rate (MIF) of 135 L/min. The bars represent the geometric mean of PF values determined under a tidal volume of 2.7 L and two PAPR flow rates of 184 and 204 L/min. The error bars represent geometric standard deviations of PF values on a log scale.

$PF_{PortaCount}$ for Hood B with the stretched elastic band. This finding indicates EPIC's efficiency in measuring relatively low protection factors.

EPIC after correction versus PortaCount

The PFs measured with the prototype EPIC after applying CFs in the algorithm, and the reference

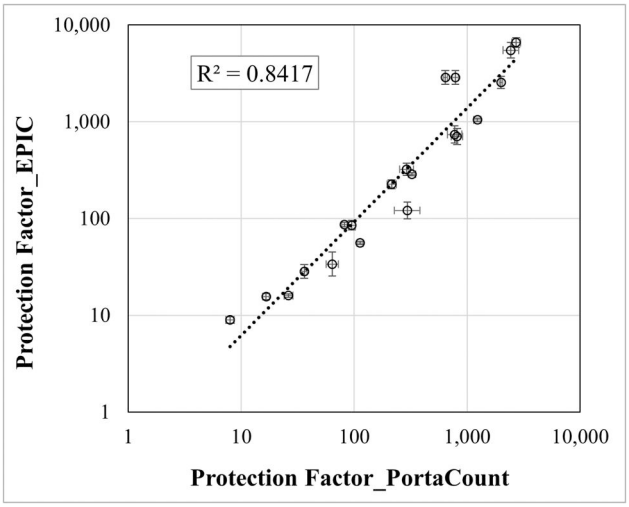

Figure 6. Respirator protection factor (PF) values measured with EPIC (after applying correction factors) *vs.* those determined with the PortaCount (reference). Each point represents the geometric mean, and the error bars represent the geometric standard deviations of PF values on a log scale.

PortaCount under all testing conditions are presented in Figure 6 as geometric means, with geometric standard deviations shown as error bars. The results demonstrated the EPIC's ability to detect the PFs over a wide range, from values below 10 to over 7,000. A correlation coefficient (R^2) of 0.84 was found between the two datasets, the tested EPIC and the reference PortaCount generated. This high correlation is appealing, as EPIC and PortaCount were based on different measurement principles and particle-size sensitivities. Deviations at high PFs occurred because the optical-based PMS-11 sensor primarily detects particles >0.3 µm, whereas the CNC-based PortaCount detects much smaller, ultrafine particles. When ultrafine particles dominated respirator leakage, the optical sensor undercounted them, potentially leading to an apparent overestimation of PF relative to CNC measurements. However, this correlation is lower than the 0.99 reported for the RePM compared with CNC devices (Grinshpun et al. 2020). One potential explanation is variation in the MIFs used during evaluation testing, which may have influenced particle counts and contributed to variability in the correlation. Additionally, EPIC showed lower data variability than the RePM, which exhibited greater variability at higher PFs.

Although both devices used the same operating principle (optical light scattering) to detect particles, they differed in their system response times. The RePM had a reaction time of 60 s, whereas the EPIC responded in less than 10 s. The EPIC's faster response may reduce fluctuations in particle counts, thereby resulting in a lower correlation coefficient than with RePM. This difference in system response time could also contribute to the observed disparities between the two devices in performance and measurement consistency. The next step in improving the EPIC will involve optimizing these data to identify the optimal response time, thereby improving the correlation coefficient.

Limitations

The optical-based PMS-11 sensor worked primarily with particles greater than 0.3 µm due to the corresponding scattering light wavelength, whereas particle sizes in healthcare environments could be as small as 150 nanometers. Particle penetration through faceseal leaks may have been undercounted by the optical sensors, creating a risk of false reassurance and overestimation of the calculated PF relative to the CNC-based device when smaller particles dominated the challenge aerosol. Therefore, it is important to understand, from a practical standpoint, the lower detection limit of optical-based sensors compared to CNC-based fit testers in real-world environments. Additionally, the PMS-11 sensor has a lower upper detection limit for high-concentration aerosols, and the results plateau above certain levels (nonlinear). The differences between inside- and outside-respirator concentrations may be compressed, further contributing to potential PF overestimation. Despite the detection limits, the EPIC prototype offered substantial advantages in cost, portability, and field-deployability, supporting its intended role as a practical, real-time monitoring tool rather than a direct replacement for laboratory CNC-based fit testing.

Conclusions

Based on the data collected in this study, the authors conclude that the prototype EPIC can effectively measure the PF of PAPRs in real time, particularly in environments with particle concentrations ranging from 40,000 to 70,000 particles/L. The EPIC shows potential for future application in quantitative performance evaluation of PAPRs. After applying CFs, the prototype EPIC demonstrated a strong correlation with the reference CPC-based method, yielding a correlation coefficient (R^2) of 0.84, which is notable given that EPIC operates on an optical light-scattering principle. The results demonstrated the EPIC's capability to monitor respirator particle ingress quantitatively. This study indicates that EPIC effectively monitored PF of PAPRs at high breathing MIF rates and high

PAPR flow rates, compared with the PortaCount fit tester. Future research should involve applying various challenge aerosols during chamber evaluations of the prototype EPIC. Additionally, the prototype EPIC should be further assessed using human-subjects-based approaches and validated in real-world workplace conditions.

Acknowledgements

The authors acknowledge the National Institute for Occupational Safety and Health (NIOSH) for providing support through a research contract (#75D30123P17111). The content is solely the authors' responsibility and does not necessarily represent the official position of NIOSH nor the Centers for Disease Control and Prevention (CDC).

Author contributions

CRediT: **Xinyi Niu**: Formal analysis, Investigation, Project administration, Validation, Visualization, Writing – original draft; **Michael Yermakov**: Data curation, Investigation, Resources, Writing – review & editing; **Matthew Horvatin**: Funding acquisition, Project administration, Resources, Supervision, Writing – review & editing; **Ziqing Zhuang**: Investigation, Resources, Supervision, Writing – review & editing; **Yang**: Investigation, Resources, Writing – review & editing; **Sergey Grinshpun**: Methodology, Resources, Supervision, Writing – review & editing; **Jun Wang**: Conceptualization, Data curation, Formal analysis, Funding acquisition, Methodology, Project administration, Resources, Supervision, Validation, Writing – review & editing.

Attribution statement

N95 and NIOSH Approved are certification marks of the U.S. Department of Health and Human Services (HHS) registered in the United States and several international jurisdictions.

Disclaimer

The findings and conclusions in this report are those of the authors and do not necessarily represent the official position of the National Institute for Occupational Safety and Health, Centers for Disease Control and Prevention. Mention of any company or product does not constitute endorsement by the National Institute for Occupational Safety and Health, Centers for Disease Control and Prevention.

Disclosure statement

No potential conflict of interest was reported by the author(s).

Funding

The work was supported by the National Institute for Occupational Safety and Health through a research contract (#75D30123P17111).

ORCID

Xinyi Niu http://orcid.org/0000-0002-3261-6382
Michael Yermakov http://orcid.org/0009-0009-5407-2695
Matthew Horvatin http://orcid.org/0000-0003-3904-6287
Ziqing Zhuang http://orcid.org/0000-0002-0771-5274
Weihua Yang http://orcid.org/0000-0002-2849-2786
Sergey Grinshpun http://orcid.org/0000-0003-4339-927X
Jun Wang http://orcid.org/0000-0003-1690-0460

Data availability statement

The data that support the findings of this study are available from the corresponding author upon reasonable request.

References

Anderson NJ, Cassidy PE, Janssen LL, Dengel DR. 2006. Peak inspiratory flows of adults exercising at light, moderate and heavy workloads. J Int Soc Respir Prot. 23:53–63.

Cohen HJ et al. 2001. Simulated workplace protection factor study of powered air-purifying and supplied air respirators. AIHAJ. 62(5):595–604. https://doi.org/10.1080/15298660108984658

Gao S et al. 2015. Penetration of combustion aerosol particles through filters of NIOSH-certified filtering facepiece respirators (FFRs). J Occup Environ Hyg. 12(10):678–685. https://doi.org/10.1080/15459624.2015.1043057

Gao S et al. 2016. Performance of an improperly sized and stretched-out loose-fitting powered air-purifying respirator: manikin-based study. J Occup Environ Hyg. 13(3):169–176. https://doi.org/10.1080/15459624.2015.1098780

Grinshpun SA et al. 2020. New respirator performance monitor (RePM) for powered air-purifying respirators. J Occup Environ Hyg. 17(11-12):538–545. https://doi.org/10.1080/15459624.2020.1814491

Haruta H et al. 2008. Experimental and theoretical investigation of the performance of N95 respirator filters against ultrafine aerosol particles tested at constant and cyclic flows. J Int Soc Respir Prot. 25:75–88.

Hinds WC. 1999. Aerosol technology: properties, behavior, and measurement of airborne particles. John Wiley & Sons.

Lafortuna CL, Minetti AE, Mognoni PIER. 1984. Inspiratory flow pattern in humans. J Appl Physiol Respir Environ Exerc Physiol. 57(4):1111–1119. https://doi.org/10.1152/jappl.1984.57.4.1111

Liverman C, Domnitz S, McCoy M. 2014. The use and effectiveness of powered air purifying respirators (PAPRs) in health care. Institute of Medicine of the National Academies of Science.

Mackey KR, Johnson AT, Scott WH, Koh FC. 2005. Over breathing a loose-fitting PAPR. J Int Soc Respir Prot. 22(1/2):1.

Mahdavi A, Bahloul A, Haghighat F, Ostiguy C. 2014. Contribution of breathing frequency and inhalation flow rate on performance of N95 filtering facepiece respirators. Ann Occup Hyg. 58(2):195–205. https://doi.org/10.1093/annhyg/met051

Mohanty A, Kabi A, Mohanty AP. 2019. Health problems in healthcare workers: a review. J Family Med Prim Care. 8(8):2568–2572. https://doi.org/10.4103/jfmpc.jfmpc_431_19

Myers WR, Peach MJ, Cutright K, Iskander W. 1984. Workplace protection factor measurements on powered air-purifying respirators at a secondary lead smelter: results and discussion. Am Ind Hyg Assoc J. 45(10):681–688. https://doi.org/10.1080/15298668491400449

Myers WR, Peach MJ, Cutright K, Iskander W. 1986. Field test of powered air-purifying respirators at a battery manufacturing facility. J Int Soc Respir Prot. 4(1):62–89.

Nicas M, Harrison R, Charney W, Borwegan B. 2004. Respiratory protection and severe acute respiratory syndrome. J Occup Environ Med. 46(3):195–197. https://doi.org/10.1097/01.jom.0000116808.46760.06

Nicholson KW. 1988. A review of particle resuspension. Atmos Environ (1967). 22(12):2639–2651. https://doi.org/10.1016/0004-6981(88)90433-7

[NIOSH] National Institute for Occupational Safety and Health. 1997. 42 CFR 84 Respiratory protective devices; final rules and notice. Federal Register 60:110.

[OSHA] Occupational Safety and Health Administration. 2006. Assigned protection factors: final rule, 29 CFR parts 1910, 1915 and 1926. Federal Register, 71 FR p. 50122–50192.

Sousan S, Koehler K, Hallett L, Peters TM. 2017. Evaluation of consumer monitors to measure particulate matter. J Aerosol Sci. 107:123–133. https://doi.org/10.1016/j.jaerosci.2017.02.013

Tellier R, Li Y, Cowling BJ, Tang JW. 2019. Recognition of aerosol transmission of infectious agents: a commentary. BMC Infect Dis. 19(1):101. https://doi.org/10.1186/s12879-019-3707-y

Vo E et al. 2015. Respirator performance against nanoparticles under simulated workplace activities. Ann Occup Hyg. 59(8):1012–1021. https://doi.org/10.1093/annhyg/mev042

Wang Y et al. 2015. Laboratory evaluation and calibration of three low-cost particle sensors for particulate matter measurement. Aerosol Sci Tech. 49(11):1063–1077. https://doi.org/10.1080/02786826.2015.1100710

Wei J, Li Y. 2016. Airborne spread of infectious agents in the indoor environment. Am J Infect Control. 44(9 Suppl):S102–S108. https://doi.org/10.1016/j.ajic.2016.06.003

Wizner K, Stradtman L, Novak D, Shaffer R. 2016. Prevalence of respiratory protective devices in US health care facilities: implications for emergency preparedness. Workplace Health Saf. 64(8):359–368. https://doi.org/10.1177/2165079916657108

Wu B, Corey J, Yermakov M, Liu Y, Grinshpun SA. 2018. Laboratory evaluation of a novel real-time respirator seal integrity monitor. Ann Work Expo Health. 62(6):742–753. https://doi.org/10.1093/annweh/wxy026

Zhai Y et al. 2018. A review on airborne microorganisms in particulate matters: composition, characteristics and influence factors. Environ Int. 113:74–90. https://doi.org/10.1016/j.envint.2018.01.007